

Distance Element Response to Distorted Waveforms

Technical Report to the Line Protection Subcommittee of the Power Systems Relaying Committee:
 K. Zimmerman, *Chair*, A. Martin, *Vice Chair*, M. Agudo, H. Ashrafi, J. Buneo, H. DoCarmo, N. Fischer,
 J. Holbach, R. Horton, K. Jones, J. Lane, Y. Liao, J. Mooney, C. Paduraru, E. Pajuelo, R. Patterson, E. Price,
 D. Sevcik, R. Turner, J. Uchiyama, J. Wang

Established: 2009;

Output: Technical Report; Completion Date: January 2013

Assignment—Write a technical report to the Line Protection Subcommittee on the performance of distance elements with distorted waveforms.

I. INTRODUCTION

Distance elements are widely used on transmission, subtransmission, and even many distribution systems. Distance-based schemes are a very economical and simple approach to protecting lines.

The performance of distance elements is based on reliable currents and voltages measured at the relay terminals, typically from current transformers (CTs) and voltage transformers (VTs). Sometimes, the power system or the instrument transformers produce a distorted waveform. These distorted waveforms can be due to CT saturation, capacitor voltage transformer (CVT) transients, or power system events such as faults on series-compensated lines, line switching, or transformer energization.

This paper studies the impact of distorted waveforms on distance-based elements, such as mho or quadrilateral elements.

The impact to the reach (underreach or overreach) and operating time are evaluated, and possible solutions are discussed.

II. DISTANCE ELEMENT DESIGN

A. Mho Distance Elements

Distance relays measure the distance to a fault on the basis of the fault loop impedance derived from current and voltage at the relay location. The measurement is done by comparing the phase relationship between an operating quantity and a polarizing quantity. The operating quantity, typically known as the line-drop compensated voltage, consists of the

measured voltage, the measured current, and the reach setting. One would typically select a polarizing quantity that would be unaffected by a fault; typical polarizing quantities for mho elements are positive-sequence voltage or unfaulted phase voltage. Equation (1) shows the typical distance element operating equation. Fig. 1 shows the vector relationship.

$$P = \text{Re}[(r \cdot Z \cdot I - V) \cdot V_p^*] \quad (1)$$

where:

P is the operating torque—positive is operate and negative is restrain.

r is set reach.

Z is replica line impedance.

I is measured current.

V is measured voltage.

V_p is polarizing voltage.

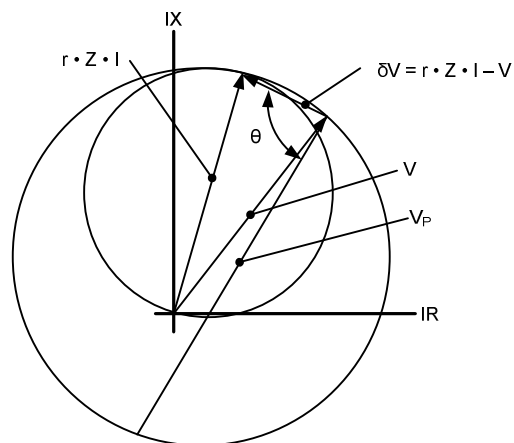


Fig. 1. Mho Element Derivation

B. Quadrilateral Distance Elements

A quadrilateral ground distance characteristic consists of four elements. Fig. 2 shows a typical quadrilateral characteristic representing the four different elements: the reactance element (top line), positive and negative resistance boundaries (right and left sides, respectively), and the directional element (bottom line). A quadrilateral ground distance characteristic operates if the measured impedance is inside the box defined by these four elements (i.e., all four elements must operate). Note that Fig. 2 depicts a typical quadrilateral element and that the shape and setting methodology for a quadrilateral element can vary greatly, and a detailed description is beyond the scope of this report.

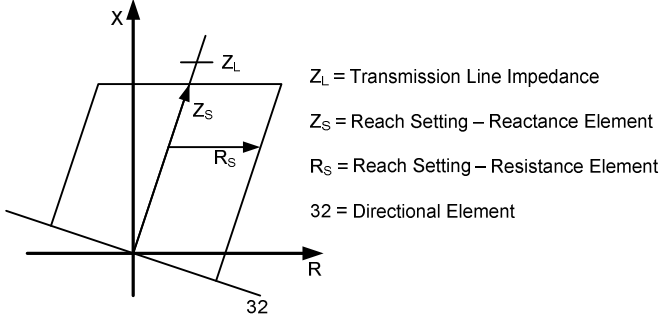


Fig. 2. Typical Quadrilateral Characteristic

The reactance element, which determines the reach along the transmission line, is polarized by current instead of voltage, as is the case with a mho element. Fig. 3 shows the derivation of the reactance measurement. When the angle between the complex conjugate of the polarizing current and the line-drop compensated voltage ($r \cdot Z \cdot I - V$) is zero, the developed torque is zero. When the torque is greater than zero, the measured impedance is below the reactance line. If it is less than zero, the measured impedance is above the reactance line. Equation (2) is a typical reactance element operating equation.

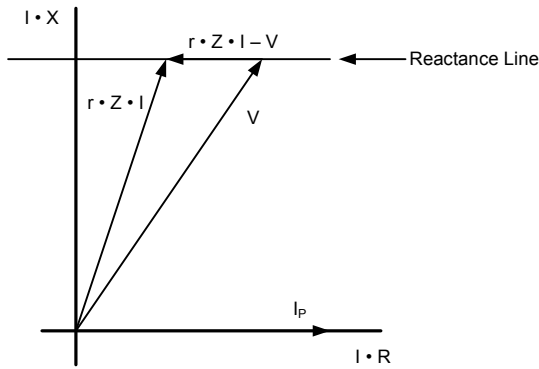


Fig. 3. Reactance Characteristic Derivation

$$Q = \text{Im} \left[(r \cdot Z \cdot I - V) \cdot I_p^* \right] \quad (2)$$

where:

Q is the operating torque; positive is operate and negative is restrain.

r is set reach.

Z is replica line impedance.

I is measured current.

V is measured voltage.

I_p is polarizing current.

Polarizing quantities for the reactance element can also vary greatly. For a quadrilateral ground distance element, a typical polarizing current would be zero-sequence or negative-sequence current. Generally speaking, phase current is a poor choice for reactance element polarization due to the influence of load flow. However, phase currents have been used in some designs.

The resistance measurement can also vary greatly with respect to methods used for calculating the measured resistance. Some designs use a simple $\text{Re}(V/I)$ measurement using the measured line to neutral phase voltage and the phase current. A resistance element using a simple V/I technique is sensitive to load flow, which may actually reduce the resistive reach of the element. Other designs use a technique that is immune to load flow and line resistance. The amount of fault resistance covered by the quadrilateral element is determined by the resistive reach setting.

The directional element is typically a zero-sequence or negative-sequence voltage polarized element, although other techniques have been used in certain designs.

C. Filtering for Distance Elements

For the distance element to provide an accurate measurement, the waveforms are filtered to extract the fundamental frequency component. The filter design may vary, but the goal is the same: to extract the fundamental frequency component of the power system waveforms. Analog low-pass filters are used to removed high-frequency components and prevent aliasing of high-frequency signals. Digital filters are used to extract the fundamental frequency component of the voltage and current waveforms. The digitally filtered values are then used as phasors in the distance relay measurement as well as overcurrent and directional elements that may be used to supervise the distance relay.

The most common digital filters are the cosine and Fourier filters. Equation (3) shows a typical implementation of a cosine filter. Equation (4) shows a typical implementation of a sine filter. A Fourier filter consists of both the sine and cosine filter, and a cosine filter consists of only the cosine portion.

$$V_f = \frac{2}{\text{SPC}} \sum_{k=0}^{\text{SPC}-1} \cos\left(\frac{k \cdot 2\pi}{\text{SPC}}\right) \cdot V_{[f-(\text{SPC}-1)]+k} \quad (3)$$

$$V_f = \frac{2}{\text{SPC}} \sum_{k=0}^{\text{SPC}-1} \sin\left(\frac{k \cdot 2\pi}{\text{SPC}}\right) \cdot V_{[f-(\text{SPC}-1)]+k} \quad (4)$$

where:

V_f is present filtered sample.

SPC is the number of samples per cycle.

D. Digital Filter Response

To better understand the filter response, we will evaluate two outputs of the digital filter: the frequency response and the

impulse response. These two responses are very useful in evaluating how the digital filter responds to transients and harmonics. The frequency response is plotted by simply applying an input signal at various frequencies and measuring the magnitude of the output. The impulse response is effectively the filter coefficient.

Fig. 4 shows the frequency response of full-cycle cosine and sine filters at 16 samples per cycle. Fig. 5 shows the filter coefficients for the same filters.

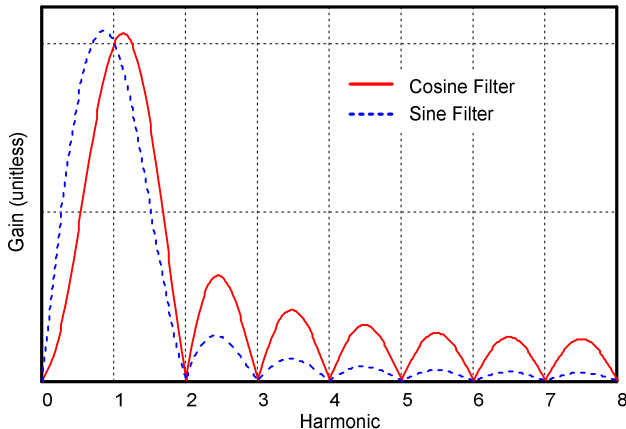


Fig. 4. Frequency Response of Full-Cycle Cosine and Sine Filters

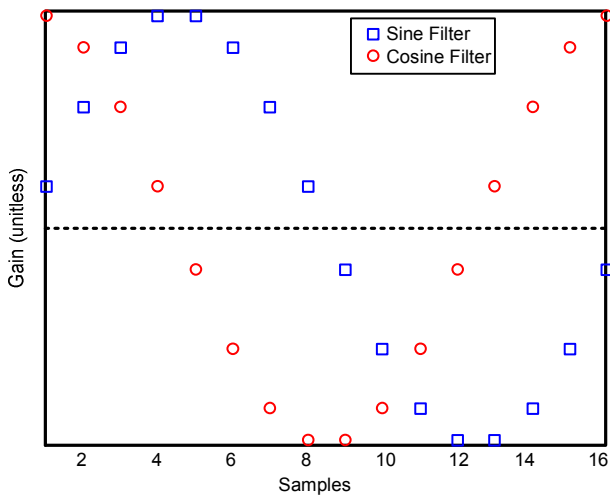


Fig. 5. Filter Coefficients

It is also interesting to evaluate the filter response to an impulse. In many ways, an impulse is representative of the currents associated with many distorted current and voltage waveforms. Fig. 6 shows the response of a full-cycle cosine filter to a single sample impulse. Note that a single sample impulse gives an output that represents an ac waveform.

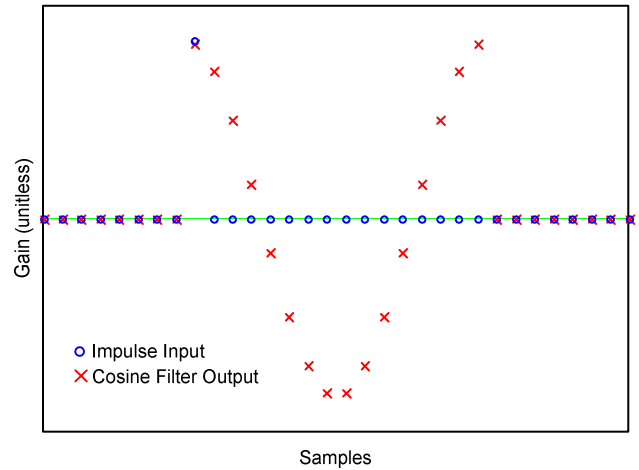


Fig. 6. Impulse Response

E. Polarizing Quantities

1) Mho Distance Elements

Mho distance elements use voltage as a polarizing reference. The polarizing voltage that is usually selected is one that is unaffected by the fault. For example, a distance element measuring the A-phase-to-ground fault loop may use the BC-phase voltage because this voltage would be relatively unaffected by an A-phase-to-ground fault. The three main categories for voltage polarization are as follows:

- Self-polarization.
- Cross-polarization.
- Positive-sequence polarization.

Self-polarization is uncommon in microprocessor-based designs but is more common in electromechanical or solid-state relay designs. A self-polarized mho element uses the same voltage as the measure fault loop (e.g., V_A for an A-phase-to-ground fault). A self-polarized mho element is unreliable for zero-voltage faults because there is no reference quantity when the measured voltage is zero. These elements can also lack directional security for reverse faults and do not provide any expansion of the mho characteristic. They are also sensitive to waveform distortion due to faults because the polarizing quantity is the faulted voltage.

Cross-polarization has been used in many distance element designs. A cross-polarized element uses a voltage that is unaffected by the fault (e.g., V_{BC} for an A-phase-to-ground fault). This method is reliable for zero-voltage faults because the polarizing voltage is unaffected by the fault. However, three-phase faults do result in unreliable operation because all three phase voltages are zero. These elements also result in an expanded characteristic that improves the resistive fault

coverage. Waveform distortion does not affect cross-polarized elements like a self-polarized element because the unaffected voltage is not typically distorted like the faulted phase voltage. This helps in directional security, but distortion of the faulted phase voltage can still result in undesired operation.

Positive-sequence voltage polarization is the most popular method used in most microprocessor-based relays. The positive-sequence voltage magnitude is high enough to use as a reliable polarizing source for all fault types except three-phase faults. For zero-voltage three-phase faults, positive-sequence polarization has the same weakness as cross-polarization. In addition, a positive-sequence voltage-polarized element has fairly reliable performance when the fault phase voltage is distorted.

The primary method for mitigating unreliable operation for three-phase faults is to use memory polarization. Memory polarization can be used in any one of the three methods described above. The advantage of memory polarization is that the distance element is directionally secure for zero-voltage three-phase faults. Note, however, that in order for the memory voltage to operate correctly, the relay requires a valid voltage for a period of time before it can be used for polarization.

2) *Quadrilateral Distance Elements*

Quadrilateral distance elements use current for the polarization of the reactance measurement. The polarizing current is typically one that is unaffected by load and is fault-induced. Phase currents are a poor choice for polarizing a reactance element because the influence of load flow on the phase current can result in severe underreach or overreach of the reactance element. Negative-sequence and zero-sequence current are excellent choices for polarization, and they are the most common polarization quantities used in modern digital relays.

Because the polarizing quantity is typically fault-induced, memory polarization is not required. However, nonhomogeneous systems can result in underreaching or overreaching of the reactance element for resistive faults. In nonhomogeneous systems, negative-sequence current may be favored because the negative-sequence network tends to be more homogeneous than the zero-sequence network.

F. *Supervising Elements*

Distance elements in microprocessor-based relays are supervised by a number of elements to improve the security and selectivity of the distance element. Typically, the same supervisory functions apply to both mho and quadrilateral distance elements. The following is a short list of common elements that are used to supervise distance elements (note that this list is not all-inclusive and that there may be other elements that are used to supervise distance elements,

depending upon the specific design philosophy):

- Fault detectors. Fault detectors (nondirectional phase or ground overcurrent elements) can be used to limit the sensitivity of a distance element to a specific current level. They are also used to prevent operation of the distance element under load conditions or when a loss-of-potential (LOP) occurs.
- Directional elements. Directional elements are typically used as secondary checks to verify that the distance element is operating for a fault in the correct direction. Although distance elements are inherently directional, there are specific applications where the distance element directionality may not be reliable.
- Faulted phase selection. Phase and ground distance elements can overreach for certain fault types (e.g., ground distance overreaches for a phase-to-phase-to-ground fault). Fault phase selection logic determines the fault type, typically identifies a fault involving ground, and enables the appropriate elements for the given fault type. In addition, proper phase selection is critical for single-pole trip applications.
- LOP. Loss of relaying potential can result in undesired operation of the distance element. All modern digital relays include logic that identifies a LOP condition that can be used to block operation of the distance element.
- Load encroachment. Nearly all modern digital relays include logic that prevents operation of the distance element under steady-state load conditions. This is useful in applications where load flow may enter the distance element characteristic.

III. APPLICATIONS

A. *Capacitive Voltage Transformer Transients*

In this section, we briefly discuss factors that affect the transient response of capacitive coupled voltage transformers (CCVT). The main focus of this section is to observe the impact that these transients have on the distance elements.

There are basically six parameters that determine the transient response of a CCVT [1]. They are as follows:

- The point on the wave when the fault occurs.
- The magnitude of the tap and the stack capacitance (C value of the stack).
- The turns ratio of the intermediate voltage transformer (step-down transformer).
- The excitation current of the intermediate transformer.
- The composition of the ferroresonance circuit (active or passive).
- The composition of the burden connected to the CCVT.

We briefly discuss the first two of these parameters in this section, but further details can be obtained in [1] and [2].

1) Point on Wave

To fully understand this phenomena, let us examine the equivalent circuit of a CCVT, as is shown in Fig. 7 [1].

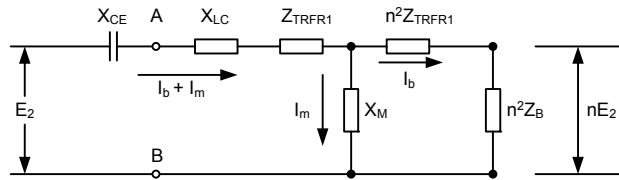


Fig. 7. The Equivalent Circuit of a CCVT With All Components Referred to the Primary Side

Fig. 8 is a sketch of the phasor relationship between the primary voltage and current and the voltages across the passive components.

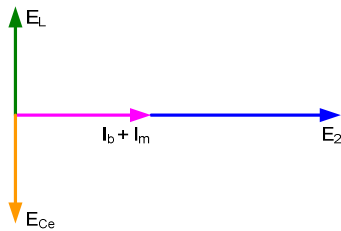


Fig. 8. Phasor Relationship Between Components of a CCVT

The burden applied to the CCVT is mainly resistive and because X_{LC} and X_M are selected such that $(X_{LC} + X_M) = X_{CE}$ at the nominal system frequency (60 Hz in the United States). This means that the passive components effectively cancel one another and the primary current ($I_b + I_m$) is in phase with the primary voltage (E_2). The voltage across the passive components is, however, 90 degrees out of phase with the primary current. In essence, the energy stored in the compensating reactor (L_C) is the same as the energy stored in the effective capacitance (C_E). The difference between the passive components is at which times each will store their maximum energy. The capacitor will store maximum energy when the primary current is minimum (voltage across the capacitor will be a maximum) and the maximum energy will be stored in the inductor when the primary current is a maximum. Because the amount of energy stored in the passive components is the same, let us examine what effect the time constants have. For this example, let us use the parameters from a 230 kV CCVT.

$$C_E = 276.9 \text{ nF}$$

$$L_C = 20.954 \text{ H}$$

$$n^2 Z_B = 110 \text{ k}\Omega$$

(5)

Using these parameters, we can now calculate the time constants of each.

$$\tau_{C_e} = n^2 Z_B \cdot C_E = 30.644 \text{ ms} \quad (6)$$

$$\tau_L = \frac{L_C}{n^2 Z_B} = 0.189 \text{ ms} \quad (7)$$

Clearly, we see that the worst-case transient occurs when we have maximum energy stored in the capacitor or when the primary voltage is at zero. Fig. 9 and Fig. 10 show the outputs of CCVT for faults that occurred at voltage zero (zero crossing) and at voltage maximum, respectively [2].

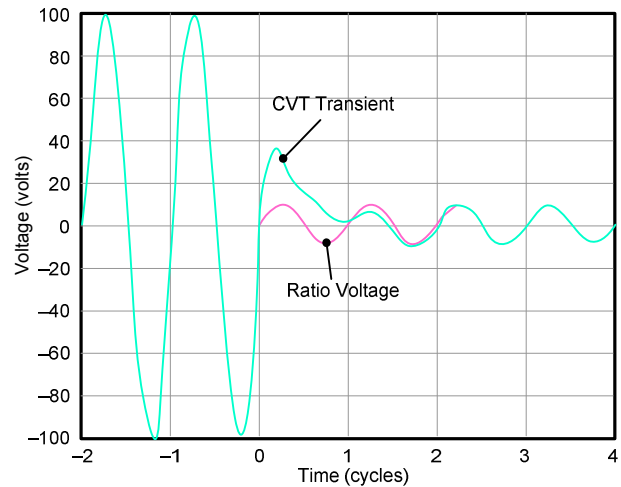


Fig. 9. CCVT Response for a Fault at Voltage Zero

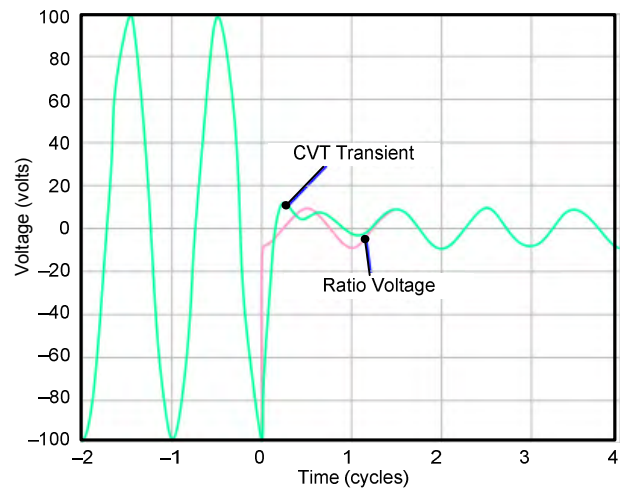


Fig. 10. CCVT Response for a Fault at Voltage Maximum

2) Magnitude of the Tap and Stack Capacitances

Again examining the equivalent circuit shown in Fig. 7, we can see that as C_E becomes larger, the capacitive reactance

becomes smaller $\left(X_{CE} = \frac{1}{2 \cdot \pi \cdot f \cdot C_E} \right)$. If the burden remains the same, the primary current will remain the same. This means that the voltage drop across the equivalent capacitance will be lower. The lower voltage will result in a lower discharge transient. Note that increasing the value of C_E may also increase the duration of the transient. Fig. 11 is a plot of the transient response of a normal value and high value capacitance CCVT [2].

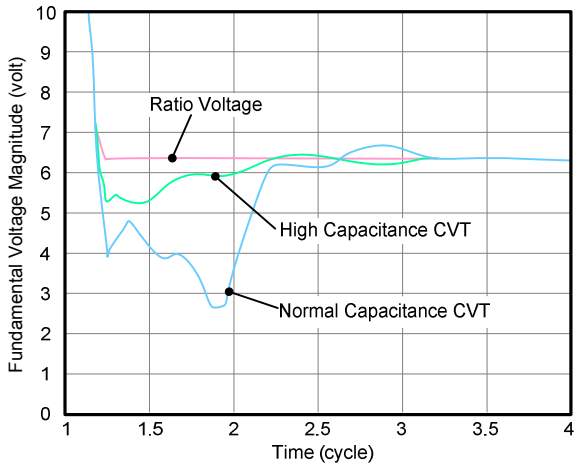


Fig. 11. CCVT Response for a Normal Capacitance CCVT and That of a High Capacitance CCVT

To show what effect a CCVT transient has on a distance relay, an actual field case is presented in this section. Fig. 12 is the oscillographic capture of the fault data, where IAW, IBW, ICW, IAX, IBX, and ICX represent the primary currents in a two-breaker line and VAY, VBY, and VCY are the primary phase voltages in kilovolts.

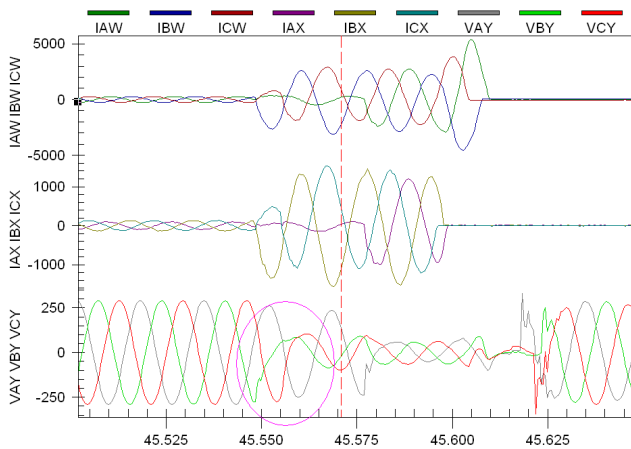


Fig. 12. Oscillographic Data

Fig. 13 is the phase-to-phase mho distance element response for the fault associated with the oscillographic data in Fig. 12.

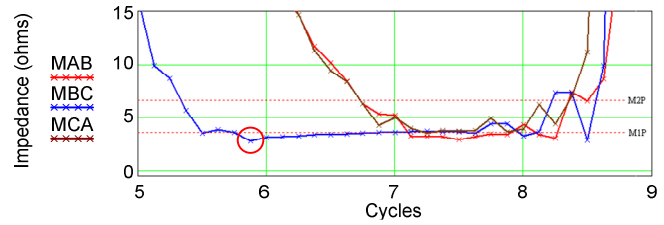


Fig. 13. Phase-to-Phase Mho Distance Element Response

From Fig. 13, we can see that CCVT transient will cause mho phase distance elements to overreach (the same is true for a quadrilateral phase distance element). In Fig. 13, the fault inception is near Cycle 5 and just before Cycle 6 we can see the apparent impedance drop below the actual fault impedance near the MIP (Zone 1) boundary point.

B. CT Saturation

Fig. 14 shows a typical waveform from CT saturation.

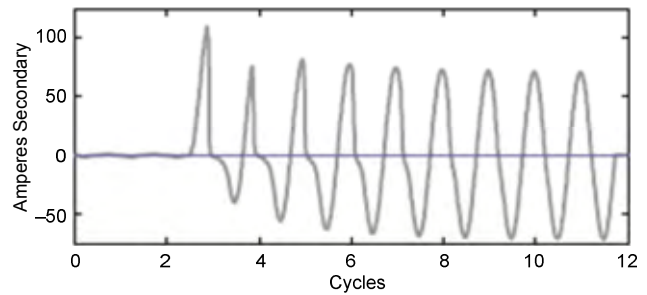


Fig. 14. Typical Waveform

The distance relay filters the waveform to extract the fundamental frequency component, as described earlier in this report. The filtered output produces phasor quantities that are used in the distance relay measurement algorithms. The CT saturation results in errors in the current measurement. In other words, the filtered output does not accurately represent the primary waveform.

The digital filter output resembles an ac waveform with a decrease in the peak magnitude as the CT goes into saturation. When the CT recovers from saturation, the peak magnitudes of the current waveform return to normal. Saturation of the CT also causes a phase shift between the unsaturated waveform and the saturated waveform. The phase shift may result in distance element underreach or overreach.

Fig. 15 shows saturated and unsaturated waveforms. Fig. 16 shows the saturated and unsaturated waveforms after digital filtering using a full-cycle cosine filter. Fig. 17 shows the magnitude of the filtered waveforms from Fig. 16. Finally, Fig. 18 shows the phase angle relationship between the saturated and unsaturated waveforms using the unsaturated waveform as a reference.

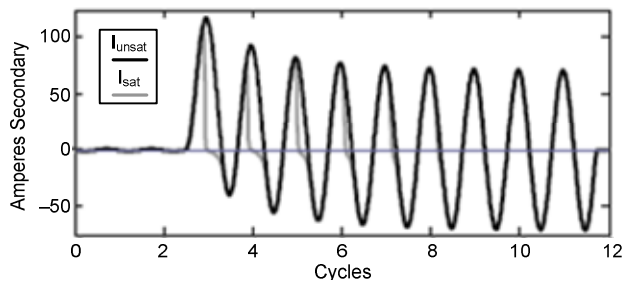


Fig. 15. Unfiltered Current Waveforms

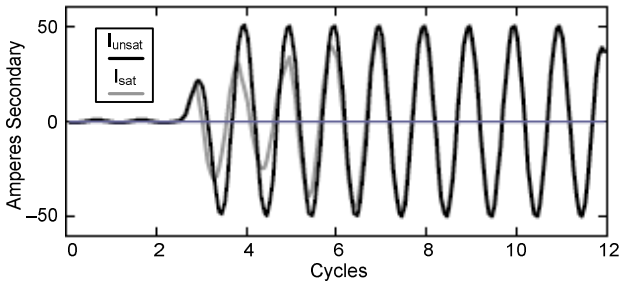


Fig. 16. Output of Full-Cycle Cosine Filter

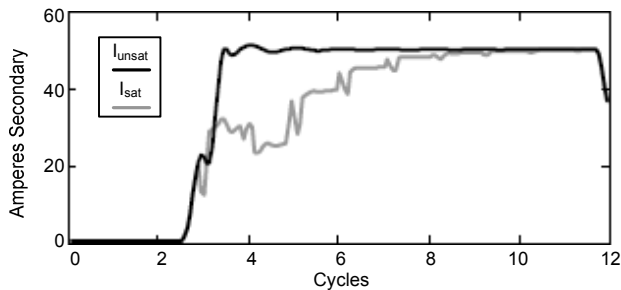


Fig. 17. Current Magnitudes With and Without Saturation

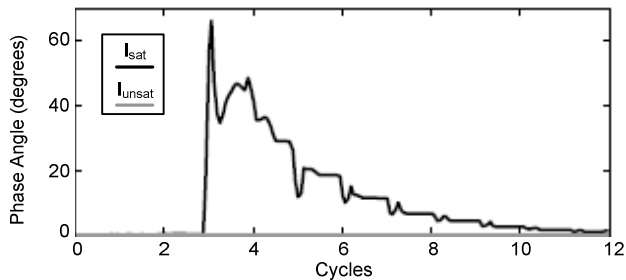


Fig. 18. Phase Relationship of Current Waveforms

We can see that the saturated current (I_{sat}) produces a lower magnitude and slightly leading phase angle compared with the unsaturated current (I_{unsat}). The result is that the distance element typically underreaches, meaning that the measured distance to the fault is greater than the actual distance to the fault. As the CT begins to recover, the distance relay measurement begins to represent the true distance to the fault. Fig. 19 shows the distance element response for a fault at about 1.8 ohms secondary. Initially, the measured impedance is correct, but as the CT saturates, the element underreaches until it is greater than the Zone 2 setting, causing a temporary dropout of the Zone 2 element. Then, as the CT comes out of saturation, the measured impedance recovers. The underreach can be problematic for pilot schemes; however, it is typically not a problem for overreaching backup functions.

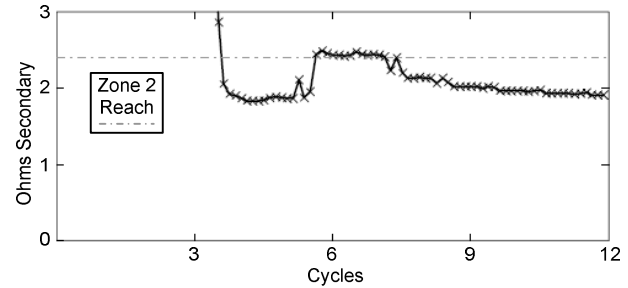


Fig. 19. Underreaching Mho Element Response

The CT saturation can also affect the relay operating time. As the saturation causes an underreach condition, it can increase the time it takes the distance element measurement to enter the operating characteristic. The impact to operating time can increase fault-clearing times by increasing the operating time for direct tripping as well as pilot tripping schemes. Fig. 20 shows the advantage of applying a high-speed Zone 1 (Z1HS) element that asserts faster than a conventional Zone 1 element that can be slowed down by CT saturation.

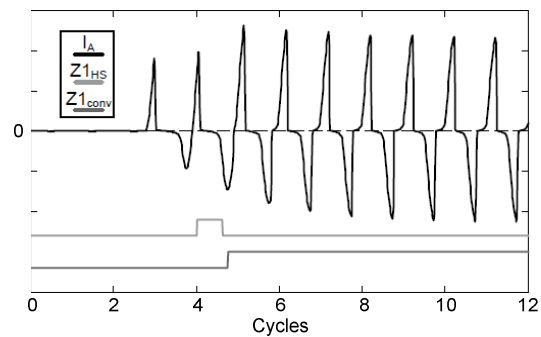


Fig. 20. Distance Element Response for Severe CT Saturation

Ideally, the CT should be sized so that it would not saturate for faults located at the remote end of the protected line. In a distance relay application, CT saturation is not a security issue, but it impacts the dependability of the protection scheme. More specifically, CT saturation can result in slow tripping of distance-based pilot protection schemes. Therefore, the CT sizing criteria is dictated by the response of the overreach Zone 2 distance element in a pilot protection scheme. The CT sizing criteria shown in (8) provides adequate margin so that a Zone 2 element used in a pilot protection scheme will operate reliably for a fault at 100 percent of the line impedance and a Zone 2 reach of 125 percent of the line impedance.

$$Z_{sb} \leq \frac{6 \cdot V_k}{\left| \frac{X}{R} + 1 \right| \cdot I_{sf}} \quad (8)$$

where:

I_{sf} is the maximum secondary fault current.

Z_{sb} is the CT burden in ohms secondary.

X/R is the X/R ratio of the fault current contribution.

V_k is the CT voltage rating.

If the connect burden is less than the right-hand side of (8), the distance element will operate correctly in terms of reach and operating time.

C. Transformer Inrush

1) Transformer Inrush Current

Transformer inrush current is a transient overcurrent that occurs during transformer energization and is caused by saturation of the magnetic core of the transformer. Inrush current is characterized by a high peak current with considerable harmonic content, particularly second-harmonic. For power transformer applications, the magnitude of the inrush current is initially two to five times the rated load current but can be somewhat greater. After the initial peak, the inrush current slowly decreases until it finally reaches the normal exciting current value that is a small fraction of 1 percent of rated load current. This decrease is the result of oscillation damping due to winding and magnetizing resistances of the transformer as well as the resistance of the system to which the energized winding is connected. This typically takes from several cycles to minutes. As a result, inrush current could be mistaken for a short-circuit current, and the transformer with bus and/or line are erroneously removed from service by protective relays. A typical single-phase inrush current waveform is shown in Fig. 21.

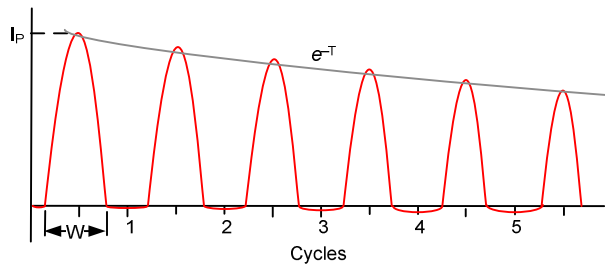


Fig. 21. Typical Transformer Inrush Current for the First Several Cycles

The inrush current peak value, I_p , harmonic content, and transient duration are dependent on the core and coil design of the transformer (i.e., magnetic characteristics, losses, winding impedances and arrangements, and so on). Fig. 22(a) is representative of the magnetic circuit characteristic of a transformer.

Using the simplified magnetizing curve of Fig. 22(b), represented by two straight line segments, OSP the instantaneous transformer excitation current, I_e , is computed using the instantaneous values of the sinusoidal flux waveform, B .

$$I_e = \frac{\sqrt{2}V_N}{R + \omega L} \left(\frac{B - B_S}{B_N} \right); B > 0 \quad (9)$$

$$I_e = 0; B < 0 \quad (10)$$

where:

V_N is applied phase-to-ground voltage at transformer terminals in volts.

L is the air core inductance of the transformer winding being energized in Henries.

R is the total dc resistance of the transformer winding being energized in ohms.

B is the instantaneous flux density of the transformer core in Teslas.

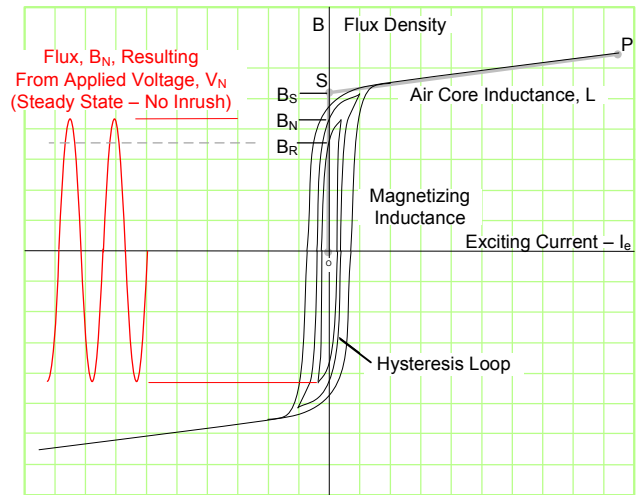
B_S is the saturation flux density of the core material in Teslas.

B_N is the normal rated flux density of the transformer core in Teslas.

B_R is the remnant flux density of the transformer core in Teslas.

I_e is the excitation current in amperes.

(a) Normal Steady-State Excitation Flux



(b) Inrush Excitation Flux

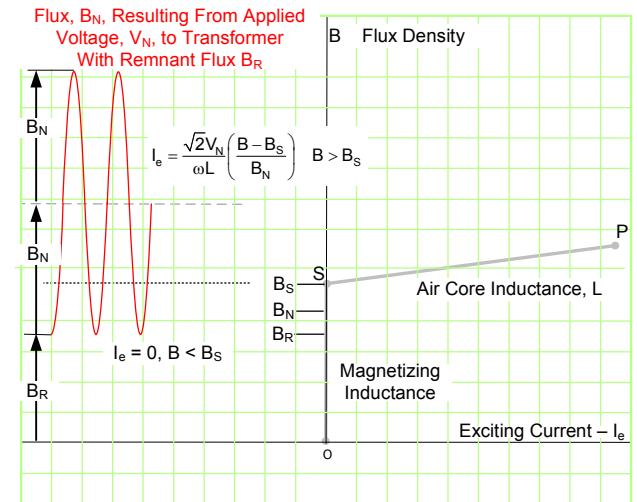


Fig. 22. Transformer Magnetizing Characteristics

The peak inrush value will occur where breaker closing occurs at the peak instantaneous flux, B , which is of opposite polarity of the maximum residual flux density, B_R . The peak inrush current is easily computed by (11), offsetting the flux density waveform by $B_R + B_N$.

$$I_p = \frac{\sqrt{2}V_N}{R + \omega L} \left(\frac{2 \cdot B_N + B_R - B_S}{B_N} \right) \quad (11)$$

The single-phase inrush current waveform, as observed in Fig. 21, is made of two components: the normal instantaneous excitation current values resulting from flux below B_S and the normal transformer exciting current, and those current values resulting from flux above B_S , the excitation inrush current that is a function of the winding's resistance and air core reactance, ωL , (the reactance of the winding when removed from the core). A point to note is that if B_R (and B_N) is equal to B_S , then the inrush current is a fully offset sine wave of fundamental frequency and would appear as a fully offset asymmetrical short circuit limited by the transformer winding's air core reactance. The inrush current waveform base width, W , would be 360 degrees (refer to Fig. 21). Practically, B_R cannot be equal to B_S , but this defines the maximum fundamental frequency component as 50 percent of the peak inrush value with the remaining 50 percent being dc. There are no harmonics. As B_R becomes a smaller percentage of B_S , the fundamental value in percent of peak decrease and the percent harmonic values increase. Generally, the highest residual flux, B_R , is assumed to be 90 percent of rated peak flux density, B_N . The saturation flux density is about 140 percent of the rated peak flux density but may go down to 120 percent (this needs confirmation with transformer manufacturers), with modern transformers using improved core steel and designs allowing higher operating induction levels.

2) Voltage at Transformer Energization

Balanced three-phase voltages are normally expected on transformer energization, even with the weakest of sources. The large magnetizing reactance (no saturation) presents basically an open circuit to the source. Also, if saturation begins to take place, lowering the impedance (air core reactance) of the transformer to the source then depending on the source impedance, the voltage at the transformer terminals would begin to reduce and likewise reduce the transformer flux that is driving the saturation. This has the effect of increasing the impedance to the source, thus raising the voltage. It is a rather instantaneous stabilization of voltage at or near the source voltage. Therefore, it is reasonable to expect balanced voltages at or near rated.

3) Current at Transformer Energization

Higher source impedances also reduce the inrush peak current as shown in (12), where V_S is the system voltage and Z_S is the source impedance. Also, the transformer winding and source resistance component of Z_S will increase the damping, and the inrush condition will decay with a faster time constant.

$$I_p = \frac{\sqrt{2}V_S}{Z_S + Z_{AC}} \left(\frac{2 \cdot B_N + B_R - B_S}{B_N} \right) \quad (12)$$

$$Z_{AC} = R + j\omega L$$

Usually, harmonic content of the inrush current is measured, and if present in sufficient quantity it is used to block operation of overcurrent and current differential functions. Historically, a 15 percent ratio of second-harmonic to fundamental content or a 20 percent ratio of total harmonic to fundamental content has been used. Harmonic analysis of

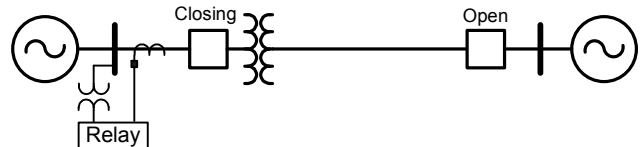
digital event recordings on modern microprocessor transformer differential relays over the past 20 years have revealed some cases where lower-than-expected harmonics were present in the inrush current waveform of one phase but not in all three phases.

To this point, we have only discussed single-phase inrush in order to simplify the analysis and increase understanding. Analysis of three-phase transformer inrush is considerably more complicated as there is an interaction between the flux in the phase cores due to the core configuration and/or winding connections. There are two simple facts that may be observed. The first is that the residual flux, B_R , is not the same polarity in all three phases of the transformer. The second is that when the transformer is energized, such that the instantaneous flux due to the applied voltage in one phase is at peak, then the flux in each of the other two phases is one half the peak value. Therefore, even in those cases of high transformer induction (B_S is less than 140 percent B_N) producing large inrush currents with low harmonics, there will be sufficient harmonics in one of the other two phase currents to ensure inrush current recognition.

4) Effects on Distance Characteristics

Transformer inrush is a well-known condition and is amply discussed as it applies to differential and overcurrent protection. The focus here, however, is on its effect on distance protection. This requires that a transformer is located within the protected zone (reach) of distance protection. Two basic system configurations that have been applied are shown in Fig. 23. These are a transmission line that is terminated into a transformer without a connecting breaker and a line with tapped transformers and their loads.

(a) Transmission Line Terminated With a Transformer



(b) Transmission Line With Tapped Transformers

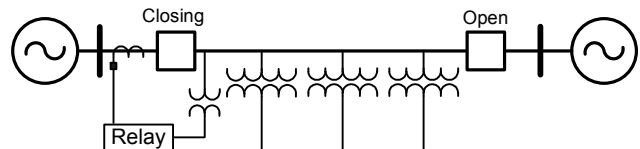


Fig. 23. Transmission Line and Transformer Configurations

The operation of distance (or impedance) relays is generally based on phase or magnitude comparators that involve the accurate measurement of the three-phase system voltages and currents. Without getting into the details of comparator operation, it is sufficient to say that filtering is employed to measure the fundamental frequency components of voltage and current as accurately as possible to ensure accurate distance unit operation. This is particularly true when using digital cosine and Fourier filters on modern microprocessor-based relays. Without sufficient study of an application, the prudent approach will be to assume the presence of fundamental current sufficient in magnitude and

duration to cause a distance unit operation. Then the issue becomes how to supervise distance units when transformers are in the protected zone. Evaluation of the transformer voltages and currents at transformer energization are required.

When applying distance protection involving transformers and inrush is a concern, then momentary blocking logic of the distance (impedance) units at transformer energization is recommended. This could be in the form of a second-harmonic restrained tripping or undervoltage supervision of distance units.

Harmonic restraint or undervoltage supervision might be considered on all distance units, including time-delayed units, to prevent operation due to extended inrush time.

D. Series-Compensated Lines

The main benefit of series-compensated lines is simple. Series capacitors are inserted into transmission lines to reduce the overall transmission reactive impedance. This benefit results in a higher power transmission capacity, higher system stability limits, better load division on parallel paths, the ability to adjust line load losses, and reduced voltage drop during severe system disturbances [3] [4].

The added capacitance to the transmission circuit contributes to a series resonance when it is combined with the impedance of the line. System disturbances will excite the system and produce high frequencies and subharmonic oscillations resulting in distorted current and voltage waveforms [4]. Shown in Fig. 24 are the current and voltage signals from a local relay of a heavily compensated line of a three-phase fault just beyond the remote bus on the line of another heavily compensated line.

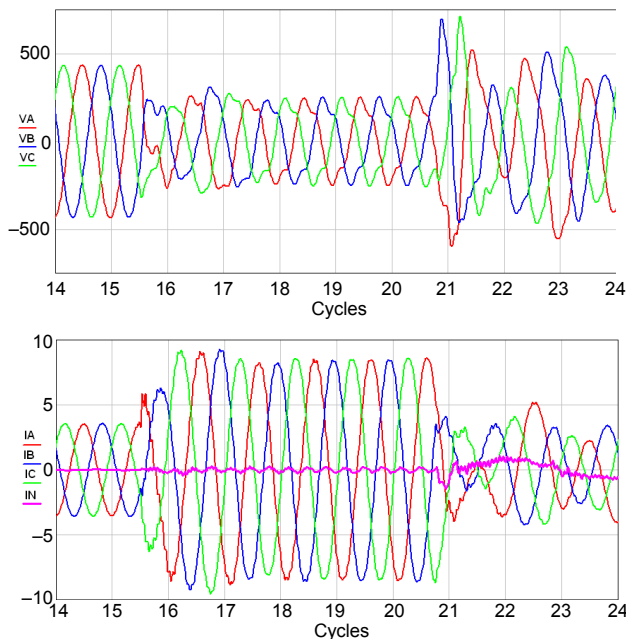


Fig. 24. Phase Fault Voltage and Current Waveforms on Series-Compensated System

Modern microprocessor-based relays attenuate high-frequency signals with analog and digital filters. Therefore they do not affect the setting or operation of distance protection elements of modern relays [5].

Subharmonic oscillations from series capacitance cause impedance measurements to oscillate. Zone 1 elements may overreach remote buses due to the spiraling nature of a fault trajectory caused by the oscillating impedance subharmonic oscillations. Impedance measurements are dependent on the overvoltage protection of the series capacitor [5].

Overreaching distance elements are susceptible to a fault appearing more resistive, and their pickup may be delayed due to the conduction of metal oxide varistors (MOVs). Modern series capacitors use MOVs with bypass breakers to provide overvoltage protection. Some of the series capacitors also include a triggered air gap, as shown in Fig. 25.

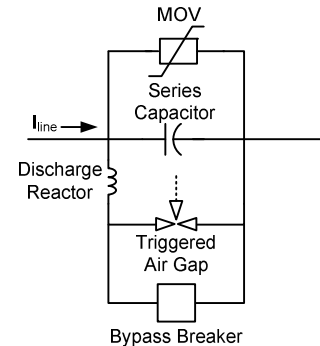


Fig. 25. Basic Circuit of an MOV-Protected Series Capacitor

When a fault current or heavy loading causes voltage across the capacitors to increase, the MOV typically limits the voltage increase to a preset level of 2 to 2.5 per unit (pu) by conducting, thus bypassing the capacitor. The MOV begins to conduct when an overvoltage threshold is reached that will change the value of the impedance of the line compensation. While the MOVs are conducting, energy is absorbed, which increases the temperature of the MOV. For some internal faults, the MOV can reach a critical temperature and require the MOV to be bypassed with a breaker. This may take as long as two cycles. If a trigger gap is included in the capacitor protection, then it may be bypassed much faster for an especially high fault current. MOVs generally do not need to be bypassed for external faults. Because the MOVs are absorbing energy, they do not remove the series capacitance in a linear fashion. MOV-protected series capacitors are challenging for the distance elements of line relays because they could be in service, bypassed by the nonlinear resistance of a MOV, or bypassed by a breaker or gap.

Consider the close-end, three-phase fault on a remote bus shown in Fig. 26.

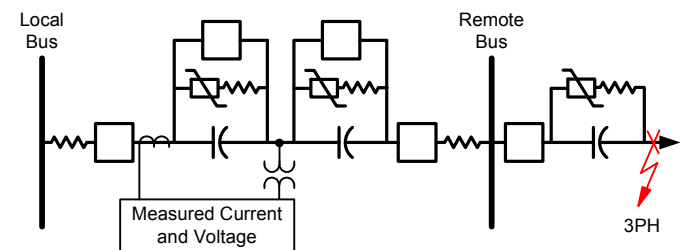


Fig. 26. Example of Heavily Series Capacitor Compensated System

Fig. 27 shows the spiraling fault trajectories of three phase-to-phase measurements of a three-phase fault on an adjacent line connected to the remote bus. The trajectories of the fault impedance are plotted with the steady-state characteristics of the local distance elements.

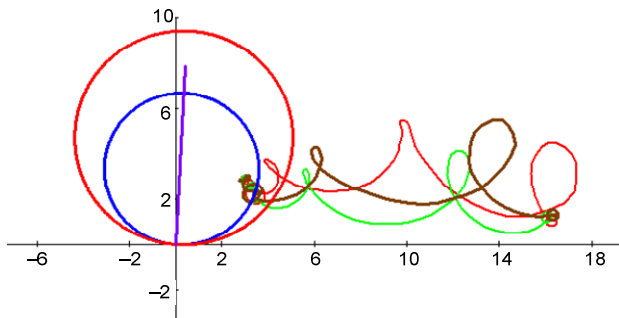


Fig. 27. Trajectories of Three Phase-to-Phase Measurements of a Three-Phase Fault

The local distance elements have typical settings, with Zone 1 set to 85 percent and Zone 2 set to 125 percent of the secondary line impedance of 7.5 ohms. The spiraling impedance trajectories caused by the subharmonic oscillations simultaneously demonstrate how the overreaching Zone 2 element may be delayed while the underreaching Zone 1 element overreaches.

To counteract effects of the subharmonic oscillations caused by series compensation, the following is recommended. For underreaching elements, set their forward reach to 70 to 80 percent of the compensated line impedance, or enable series compensation logic if the relay supports it, and set the reach to manufacturer recommendations. For overreaching elements used in transfer trip schemes, set the elements to 175 to 200 percent of the noncompensated line impedance to ensure high-speed tripping.

E. The Impact of Ferroresonance

Ferroresonance is a general term used to describe a variety of resonant interactions between capacitors and saturable iron-core inductors. During resonance, the capacitive and inductive currents are in opposition. As a result, the current is limited only by the system resistance, thus causing unusually high voltages and/or currents. The most common conditions in which ferroresonance can occur are the following:

- Transformer is accidentally supplied on one or two phases.
- Transformer is energized through the grading capacitance of one or more open circuit breakers.
- Transformer is connected to a series-compensated transmission line.
- Voltage transformer is connected to an isolated neutral system.
- Transformer is connected to a de-energized transmission line running in parallel with one or more energized lines.

- Transformer is supplied through a long transmission line or cable having low short-circuit power.
- Nonlinear loads are connected to a secondary winding of a capacitive voltage transformer.

The most common solution to mitigate the effects of ferroresonance is to install damping resistors on the secondary of station power transformers or on the VT secondaries. The limitation of the latter method is that the additional load drastically reduces the available power for the rest of the connected equipment (i.e., meters, relays, and so on). Regardless of the condition that created the ferroresonance, the disturbance will often affect the performance of protective relays and thus needs to be analyzed prior to commissioning equipment. The following presents a study of ferroresonance that occurred due to undersized auxiliary VTs being connected to a CCVT.

Auxiliary VTs are used to provide isolation or to connect various equipment rated at a voltage that differs from the source. Upon switching or high-speed reclosing, a transient overvoltage up to twice the nominal voltage may be measured on the secondary of a CCVT. If the auxiliary VT (a saturable inductor) is not sized appropriately, it will saturate, thereby triggering ferroresonance. Ferroresonance produces higher harmonics and subharmonics that distort the waveform significantly. The problematic harmonics in this situation are typically a submultiple of the nominal frequency. For example, a nominal frequency of 60 Hz will display harmonics at 20 or 30 Hz. Subharmonic content will overexcite the VT iron cores of the auxiliary VTs, driving them into saturation and thus overloading the voltage circuit. When these harmonics saturate the auxiliary VTs, it is common for protective elements in the circuit (e.g., fuses or mini-circuit breakers) to trip, leaving electromechanical distance relays with no restraint quantity. With no restraint quantity and in the absence of fault detectors, these relays are subject to misoperation.

The CCVT manufacturers are well aware of the effects of ferroresonance. All CCVTs are designed with a ferroresonance suppression circuit. These suppression circuits can be either active (sparking gaps which arc over when the voltage exceeds a specific threshold) or passive. The passive suppression circuit offers better transient response than the active suppression circuit. The passive approach employs a saturable inductor to draw a higher current that, in turn, increases the voltage drop across a reactor. This voltage will spark a gap that drains the energy to ground via a damping resistor. That drain effect is usually complete in less than 10 cycles.

CCVT manufacturers also specify that the auxiliary VTs, if connected to the same source as the protective relays (can be a different winding though), need to be selected so that the iron core is supplied with less than one half the flux density required to reach the knee of the magnetization curve. For example, they recommend employing a 230 V/230 V auxiliary VT in the 115 V circuit rather than a unit rated 115 V/115 V.

Fig. 28 is a graph of the excitation current for several types of auxiliary VTs considered to mitigate the effects of ferroresonance.

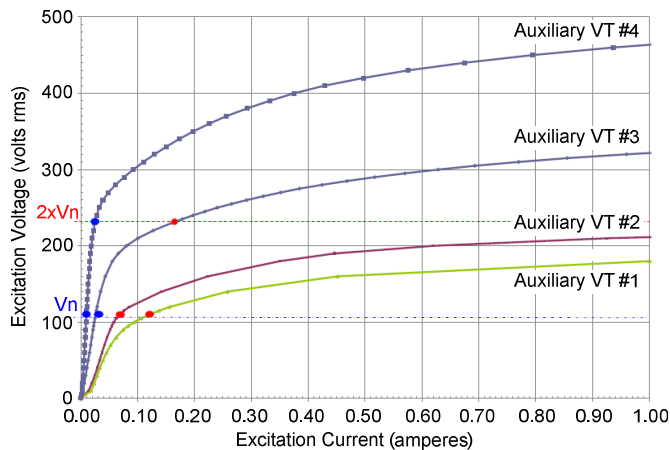


Fig. 28. Excitation Characteristics for Several Types of Auxiliary VTs

Anytime the operating point (that is the intersection between the maximum level of the voltage supplied and the excitation curve) is beyond the knee point, the system will likely go into ferroresonance. If Auxiliary VT #1 is employed, the ferroresonance will be sustained—that is, the damping circuit of the CCVT may not be efficient and the ferroresonance may continue to stress the equipment connected to the secondaries of the CCVT. For this specific type of auxiliary VT, ferroresonance may be triggered by even applying a quantity on the upper range of the operating voltage (10 percent higher, for instance).

Auxiliary VT #2 has similar characteristics as Auxiliary VT #1. The difference resides on the quality of the iron core material.

If Auxiliary VT #3 (double flux density) is used, ferroresonance is not likely to occur. Even though the characteristic is linear at the nominal voltage, this type of auxiliary VT may go into saturation when twice the nominal voltage is applied as a result of switching the line out and back in.

In order to be sure that the auxiliary VTs are not the culprit for a potential ferroresonant condition, a transformer with a characteristic similar to Auxiliary VT #4 should be used. This transformer is built to have a linear characteristic up to twice the rated voltage.

Modern microprocessor-based distance relays have embedded logic to block the operation in case of LOP (which can occur due to overloading the auxiliary VTs and CCVTs during ferroresonance). A ferroresonant condition will not result in a misoperation once the voltage circuit is disconnected from the source (on overload condition as specified previously). Nevertheless, the distorted waveform created by ferroresonance can have a significant impact on the performance of the relay.

Fig. 29 is a record from a distance relay that overreached for an out-of-section fault. The ferroresonance condition was already present when the fault occurred.

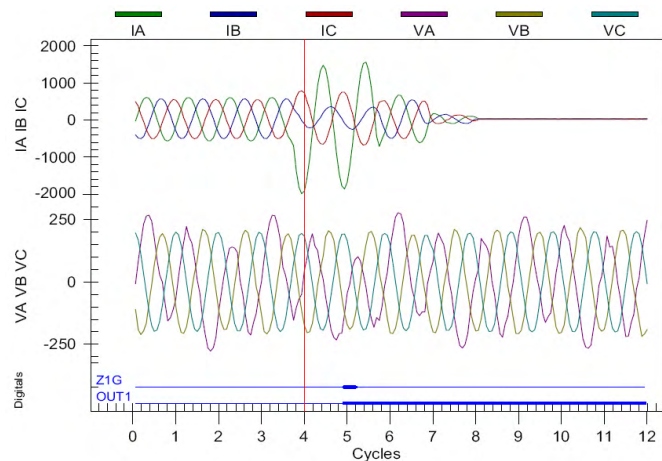


Fig. 29. Relay Overreach for an Out-of-Section Fault

For this example, the system frequency (60 Hz) and the relay sampling frequency (58.5 Hz) did not match. The sampling frequency was different because of the subharmonic frequency (20 Hz) superimposed to the fundamental frequency due to ferroresonance. The relay switched to the long memory time constant and froze the polarizing memory. The measured voltage and the polarizing voltage began to drift apart and consequently the relay tripped. It is therefore critical to size the auxiliary VTs properly. For this particular example, the auxiliary VTs were used to provide adequate voltage to the synchroscope. It is a common mistake to assume that an auxiliary VT can ride through any transient produced by switching equipment (e.g., lines, transformers, and so on). As a matter of fact, the undersized auxiliary VTs may be the culprit for producing a sustained ferroresonance. The question is not if the auxiliary VT can handle the voltage surge. The relevant question is what type of auxiliary VTs should be designed and chosen correctly to avoid ferroresonance from the beginning.

Care must be exercised when auxiliary VTs are required in the voltage circuit. Employing adequate potential/voltage transformers is critical to avoid ferroresonant conditions. A sustained ferroresonance will eventually lead to system outages and to equipment failure (e.g., CCVTs, auxiliary VTs, protective relays, metering equipment, and so on), reducing the overall reliability of the system and significantly increasing the cost of maintaining it.

F. Transients Due to Faults

This section illustrates the transient phenomena caused by short-circuit faults in a power system that may affect distance protection. When a fault occurs, the system changes from one state to another state, thus generating transients due to the presence of inductive and capacitive components in the

circuit. The most common transients include high-frequency transients in voltage and current signals with dc offset, which decays with time in the current signals. Fig. 30 shows example waveforms during a three-phase fault on a 500 kV transmission line.

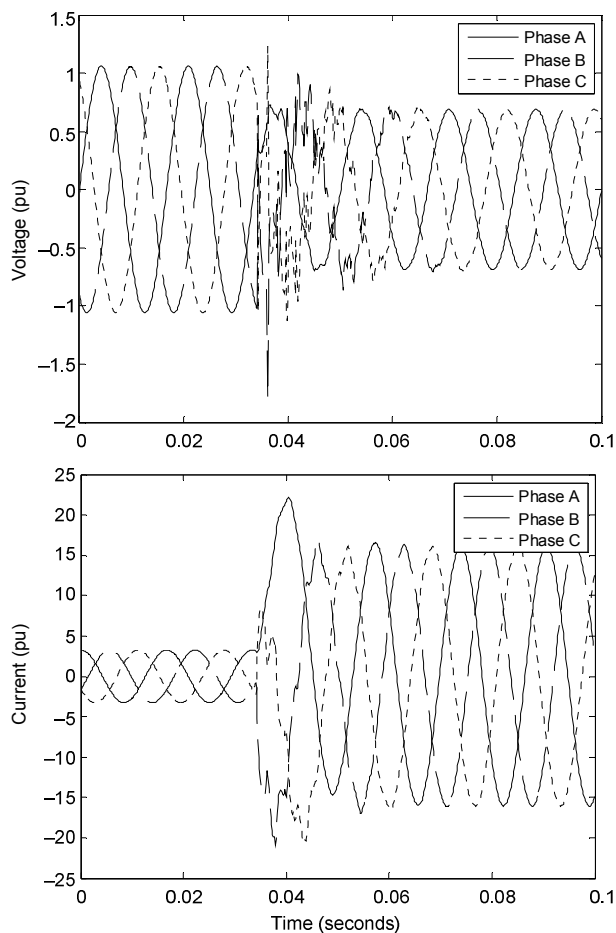


Fig. 30. Example Voltage and Current Waveforms During a Three-Phase Fault

It can be seen that both voltage and current signals are distorted by high-frequency transients. Beyond that, the current signals also contain dc decaying components, which are most apparent in the Phase A current in this particular example.

A distance relay usually employs fundamental frequency voltage and current phasors to calculate the apparent impedance or fault distance to decide the zone where a fault belongs. The phasors are extracted from the captured waveforms. Errors in extracted phasors can cause either overreach or underreach. Therefore, accurately extracting phasors from distorted waveforms is pivotal in ensuring the performance of a distance relay [3] [6].

Fundamental frequency phasors usually can be obtained using two methods [6]. In the first method, a low-pass filter such as a Butterworth filter is applied to the distorted signals to remove the high-frequency components, and then the Fourier transform is used to calculate the phasors. However, the accuracy of this method is adversely affected by dc components. In the second method, the signals are first

processed through a low-pass filter. Then the least-squares-based method is adopted to estimate the fundamental frequency phasors as well as certain high-frequency components that may be of interest for protection purposes [8]. In this method, a signal model is assumed and then a set of equations are established based on the model and measured voltage and current samples. Generally, there are more equations available than the number of unknowns, so the least-squares approach can be harnessed to derive the phasors. This method can accurately estimate the needed phasors and completely remove the dc component as long as the assumed signal model is true.

It is noted that not all distance relaying algorithms make use of phasors to decide where the fault is. In some approaches, the instantaneous values of the voltages and currents are directly used to pinpoint the fault location, obviating the need to estimate the voltage and current phasors. Instead of removing the high-frequency transients and dc components, this type of algorithm takes advantage of them to make a sound decision. The key idea is that differential equations are established to link the relationship between the measured voltage and current samples, the line parameters, and the fault distance. Solving the equations can yield the fault distance.

Another method that harnesses high-frequency transients is derived from the traveling wave theory [6]. This approach is based on the speed of the traveling wave created by a fault and the time it takes for the wave to reach the local relay and the time it takes the wave reflected from the remote terminal to reach the local relay. The essential step is to accurately identify the moments when the traveling waves reach the local substation based on the signatures found in the transient voltage and current signals.

IV. REFERENCES

- [1] A. Sweetana, "Transient Response Characteristics of Capacitive Potential Devices," *IEEE Transactions on Power Apparatus and Systems*, Vol. PAS-90, Issue 5, September 1971, pp. 1989–2001.
- [2] D. Hou and J. Roberts, "Capacitive Voltage Transformers: Transient Overreach Concerns and Solutions for Distance Relaying," proceedings of the Canadian Conference on Electrical and Computer Engineering, Calgary, AB, Canada, May 1996. Available: <http://www.selinc.com>.
- [3] J. Blackburn, *Protective Relaying Principles and Applications*. Second Edition. Dekker, New York, NY, 1998.
- [4] G. Alexander, J. Andrichak, S. Rowe, and S. Wilkinson, "Series Compensated Line Protection – A Practical Evaluation," proceedings of the 16th Annual Western Protective Relay Conference, Spokane, WA, October 1989.
- [5] H. Altuve, J. Mooney, and G. Alexander, "Advances in Series-Compensated Line Protection," proceedings of the 35th Annual Western Protective Relay Conference, Spokane, WA, October 2008.
- [6] A. G. Phadke and J. S. Thorp, *Computer Relaying for Power Systems*, John Wiley & Sons Ltd, Chichester, West Sussex, England, 2009.
- [7] F. Anderson and W. Elmore, "Overview of Series-Compensated Line Protection Philosophies," proceedings of the 17th Annual Western Protective Relay Conference, Spokane, WA, October 1990.
- [8] M. S. Sachdev and M. A. Baribeau, "A New Algorithm for Digital Impedance Relays," *IEEE Transactions on Power Apparatus and Systems*, Vol. 98, Issue 6, November 1979, pp. 2232–2240.